Clinical Radiology 74 (2019) 325.e1–325.e8

Contents lists available at ScienceDirect

Clinical Radiology

journal homepage: www.clinicalradiologyonline.net

Diffusion-weighted imaging of the kidney: comparison between simultaneous multi-slice and integrated slice-by-slice shimming echo planar sequence

G. Zhang [a], H. Sun [a,*], T. Qian [c], J. An [c], B. Shi [d], H. Zhou [a], Y. Liu [a], X. Peng [b], Y. Liu [b], L. Chen [b,***], Z. Jin [a,**]

[a] *Department of Radiology, Peking Union Medical College Hospital, Peking Union Medical College and Chinese Academy of Medical Sciences, Beijing, China*
[b] *Department of Nephrology, Peking Union Medical College Hospital, Peking Union Medical College and Chinese Academy of Medical Sciences, Beijing, China*
[c] *MR Collaboration, Siemens Healthcare Ltd, Beijing, China*
[d] *Department of Radiology, Shenzhen Sun Yat-Sen Cardiovascular Hospital, No. 1021 Dongmen Road North, Luohu District, Shenzhen, China*

ARTICLE INFORMATION

Article history:
Received 7 July 2018
Accepted 11 December 2018

AIM: To compare the simultaneous multi-slice (SMS) and integrated slice-by-slice shimming (iShim) single-shot echo planar imaging (ssEPI) for diffusion-weighted imaging (DWI) of the kidneys.

MATERIALS AND METHODS: In this prospective study, six healthy volunteers and 22 patients with renal diseases underwent SMS and iShim DWI of the kidney with five b-values (0, 80, 400, 800, 1,600 s/mm^2) at 3 T. The subjective image quality, signal-to-noise ratio (SNR), contrast-to-noise ratio (CNR), and ADC values were evaluated. The subjective image quality scores, SNR, CNR, ADC values and scan time of SMS and iShim DWI were compared.

RESULTS: Scan time of SMS DWI (1 minute 38 seconds) was significantly reduced compared to iShim ssEPI (3 minutes 33 seconds). No statistically significant differences in the SNR or subjective image quality were observed on the b=0 images, but the SNR and overall image quality scores were significantly higher on the other four b-value images at SMS DWI. Image distortions were also comparable, but there were fewer artefacts on the b=80 and b=800 images in SMS DWI. CNR was significantly higher on the b=0 and b=1,600 images in SMS DWI. SNR and subjective image-quality scores of ADC maps were significantly higher in SMS DWI, whereas CNR showed no significant difference. The ADC value of renal parenchyma was similar in SMS and iShim DWI ($1.54\pm0.11 \times 10^{-3}$ versus $1.52\pm0.16\times10^{-3}$ mm^2/s, p=0.343).

* Guarantor and correspondent: H. Sun, Department of Radiology, Peking Union Medical College Hospital, Peking Union Medical College and Chinese Academy of Medical Sciences, ShuaiFuYuan 1#, WangFuJing Street, Dongcheng District, Beijing, 100730, China.
** Guarantor and correspondent: Z. Jin, Department of Radiology, Peking Union Medical College Hospital, Peking Union Medical College and Chinese Academy of Medical Sciences, ShuaiFuYuan 1#, WangFuJing Street, Dongcheng District, Beijing, 100730, China.
*** Guarantor and correspondent: L. Chen, Department of Nephrology, Peking Union Medical College Hospital, Peking Union Medical College and Chinese Academy of Medical Sciences, ShuaiFuYuan 1#, WangFuJing Street, Dongcheng District, Beijing, 100730, China.
E-mail addresses: sunhao_robert@126.com (H. Sun), chenlpumch@163.com (L. Chen), jinzy@pumch.cn (Z. Jin).

https://doi.org/10.1016/j.crad.2018.12.005

CONCLUSION: SMS can substantially reduce imaging time of kidney DWI with slightly improved image quality and comparable ADC values of renal parenchyma compared to iShim ss-EPI sequence.

Introduction

Kidney disease and cancer are very common with an increasing global burden in the last few decades.[1,2] Among commonly practiced imaging techniques, magnetic resonance imaging (MRI) has the ability to monitor changes in morphology and function of the kidney non-invasively.[3] Clinical MRI protocols for kidney evaluation usually include T2-weighted (W) fast spin echo, T1W gradient recalled echo (GRE) in/out of phase imaging, three-dimensional (3D) fat-suppressed spoiled GRE T1W sequences before and after gadolinium injection, and optional diffusion-weighted imaging (DWI) sequences.[4] DWI, which is a standard MRI sequence in neuroimaging, has become increasingly important for evaluating kidney diseases.[5–7] Recently, DWI has found a variety of applications including characterisation of renal function and differentiation of renal tumors,[8–11] but DWI has not yet become part of most clinical routine kidney protocols because of lack of standardised acquisitions and relatively long acquisition times.[12]

As multi-b-value DWI has become popular in practice, scan time reduction is critically important for promoting routine application of kidney DWI. Simultaneous multi-slice (SMS) data acquisition has been introduced in recent years and it has been proved to successfully shorten acquisition time of DWI in the prostate, liver, breast, and pancreas.[13–16] As for the kidney, in comparison to the most common image formation technique for DWI,[17] single-shot echo planar imaging (ss-EPI), SMS DWI with the blipped-controlled aliasing in parallel imaging results in higher acceleration (CAIPIRINHA) technique[18] has been demonstrated to substantially reduce scan time.[12] Meanwhile, SMS DWI can maintain image quality and apparent diffusion coefficient (ADC) quantification accuracy when an acceleration factor (AF) of 2 is used, but this results in compromised image quality and ADC quantification accuracy if an AF3 is applied.[12] Another technique, integrated slice-by-slice shimming (iShim) technique, which is designed to improve the image quality in regions with strong susceptibility by dynamically adjusting optimised shim settings for each slice in a multi-slice acquisition, has also been reported to moderately decrease scan time compared to the conventional 3D shim technique.[19] Besides, by optimising B_0 homogeneity, iShim could overcome the drawback of ss-EPI, which is the sensitivity to B_0 inhomogeneity resulting in image distortion and negatively impacting spatial resolution. Several studies have shown that the iShim technique reduces artefacts and improves image quality of the neck[20] and whole-body DWI[19] compared to conventional ss-EPI. To the authors' knowledge, no published studies have evaluated the potential of using the iShim ss-EPI technique for kidney DWI.

As the SMS technique could substantially reduce imaging time without compromising image quality and the iShim technique is supposed to improve image quality while mildly shortening the scan time compared to a standard shim mode, the present research question was which one of the two techniques would be more appropriate for kidney DWI with faster acquisition and better image quality. Therefore, the purpose of the present study was to compare the performance of SMS and iShim ss-EPI techniques for kidney DWI in terms of scan time, image quality, and ADC quantification accuracy.

Materials and methods

Patient selection

The Institutional Review Board approved this prospective study and all the participants gave written informed consent. Between March 2017 and July 2017, six healthy volunteers (three men, three women; mean age, 29.1±6.2 years) and 24 consecutive patients (15 men, nine women; mean age, 42.3±14.4 years) who attended the nephrology outpatient clinic were recruited for the study. Two of the 24 patients were excluded as they felt claustrophobic and unable to complete the examination. As a result, a total of 28 participants (17 men, 11 women; mean age, 39±13 years) completed the MRI without reporting any discomfort. All the healthy volunteers had a normal estimated glomerular filtration rate (eGFR >90 ml/min/1.73m^2) and no history of any kidney disease or surgery. Of the 22 patients, seven patients had a histologically confirmed diagnosis of IgA nephropathy, four patients were genetically diagnosed as having Gitelman syndrome, two patients had chronic kidney disease (CKD) with malignant hypertension (stage 3, n=1; stage 4, n=1) and nine patients had CKD with chronic glomerulonephritis (stage 3, n=3; stage 4, n=3; stage 5, n=3). The four patients with Gitelman syndrome had normal renal function (eGFR >90 ml/min/1.73m^2) and the rest of 18 patients had impaired renal function (eGFR <90 ml/min/1.73m^2).

MRI protocol

All DWI data were acquired on a MAGNETOM Skyra 3T MRI system (Siemens Healthcare, Erlangen, Germany) using

an 18-channel phase-arrayed body coil in combination with part of a 32-channel spine coil. Axial DWI of the kidney was performed with both prototypic SMS-DWI sequence and prototypic iShim ss-EPI sequence. Detailed acquisition parameters of the two sequences were summarised in Table 1. For the purpose of fat saturation, spectral attenuated inversion recovery (SPAIR) technique was used in SMS-DWI. As the radiofrequency pulses of SPAIR are non-selective and applied on the whole volume, SPAIR does not allow for slice-specific shimming. Thus, fat saturation was performed with water excitation using a slice-selective pulse[21] in iShim ss-EPI DWI. The SMS sequence used the blipped-CAIPIRINHA unaliasing technique and the slice-generalised auto-calibrating partially parallel acquisition (GRAPPA) reconstruction technique. ADC maps were calculated automatically by each sequence. Scan time was recorded for each DWI sequence and compared between SMS-DWI and iShim ss-EPI DWI.

Image analysis

All the images were transferred to a workstation for post-processing using dedicated software (syngo.via; Siemens Healthcare, Erlangen, Germany). Images were de-identified and arranged randomly before being accessed by the reviewers.

Qualitative image analysis

Two radiologists with 3 and 11 years of experience in abdominal MRI evaluated the image quality of five b-value images (0, 80, 400, 800, 1,600 s/mm^2) and corresponding ADC maps independently. The two radiologists were blinded to the sequence information. A five-point Likert scale was used by the reviewers to rate the overall image quality (5=excellent, 4=good, 3=moderate, 2=poor, 1=not diagnostic), occurrence of artefacts (5=no artefact, 4=mild, 3=moderate, 2=severe, 1=not diagnostic), and distortion (5=no distortion, 4=mild, 3=moderate, 2=severe, 1=not diagnostic). The average scores of subjective image quality parameters of SMS and iShim DWI sequences for each radiologist were calculated.

Table 1
Summary of SMS and iShim DWI sequence parameters.

Sequence parameters	SMS DWI	iShim DWI
Sequence	ss-EPI	ss-EPI
Breathing scheme	Free-breathing	Free-breathing
TR (ms)	3,000	6,400
TE (ms)	66	64
FOV (mm^2)	400×325	400×325
Matrix	128×73	128×73
Section thickness (mm)	4.0	4.0
Sections	30	30
Bandwidth per pixel (Hz)	1,954	2,298
Voxel size	1.6×1.6×4.0	1.6×1.6×4.0
Ipat	GRAPPA2+SMS2	GRAPPA2
No. of ref lines for GRAPPA	42	42
Fat saturation	SPAIR	Water excitation
Diffusion mode	3-scan trace	3-scan trace
Shim mode	Standard	iShim
Interpolation	On	On
Concatenations	1	1
b-Values (averages), s/mm^2	0 (1), 80 (1), 400 (2), 800 (4), 1,600 (4)	
AF	2×2	2
Image filter (intensity/edge enhancement/smoothing)	On (smooth/1/5)	On (smooth/1/5)
Total acquisition time	1 min 38 s	3 min 33 s

SMS, simultaneous multi-slice; iShim, integrated slice-by-slice shimming; DWI, diffusion weighted imaging; TR, time of repetition; TE, echo time; FOV, field of view; iPAT, integrated parallel acquisition technique; GRAPPA, generalised autocalibrating partially parallel acquisition; SPAIR, spectral presaturation attenuated inversion recovery; AF, acceleration factor.

Quantitative image analysis

To obtain objective image parameters, the signal-to-noise ratio (SNR), contrast-to-noise ratio (CNR), and ADC values of SMS and iShim DWI sequences were evaluated. All measurements were derived from one single slice per scanned patient. The SNR was defined as the ratio between the mean signal intensity of the kidneys (S_{kidney}) and the standard deviation of background noise ($SD_{background}$) according to the following equation:

$$\mathrm{SNR} = \frac{S_{kidney}}{SD_{bacground}}$$

The CNR was defined by the following equation:

$$\mathrm{CNR} = \frac{\left|S_{kidney} - S_{muscle}\right|}{\sqrt{SD_{kidney}{}^2 + SD_{muscle}{}^2}}$$

where S_{muscle} represented the mean signal intensity of the psoas muscle, SD_{kidney} and SD_{muscle} represented the standard deviation of the kidneys and psoas muscle.

Regions of interest (ROIs) were manually placed on the b=0 images, the ROIs for the kidneys were delineated carefully within the margin of renal parenchyma at the level of renal hilum and the ROIs for muscle were drawn within the same slice as shown in Fig 1. As noise was not uniformly distributed in the background due to parallel acquisition, ROIs for background noise were drawn outside the body over the whole background instead of small ROIs placed in certain region of the background. The copy and paste function of the post-processing software allowed ROIs to be placed at the same level and position in both SMS and iShim sequences for all b-value images and corresponding ADC maps. The consistency in sizes and shapes of ROIs across patients was maintained as much as possible. The mean value, standard deviation, and size of each ROI were recorded and all the measurements were performed twice by two radiologists independently, both of them with 3 years of experience in abdominal MRI. The average of SNRs, CNRs, and ADC values were compared between SMS and iShim sequences.

Statistical analysis

All statistical analyses were performed by using SPSS 22.0 (IBM SPSS Statistics, version 22, IBM Corp, Somers, NY, USA). A $p<0.05$ was considered statistically significant. To

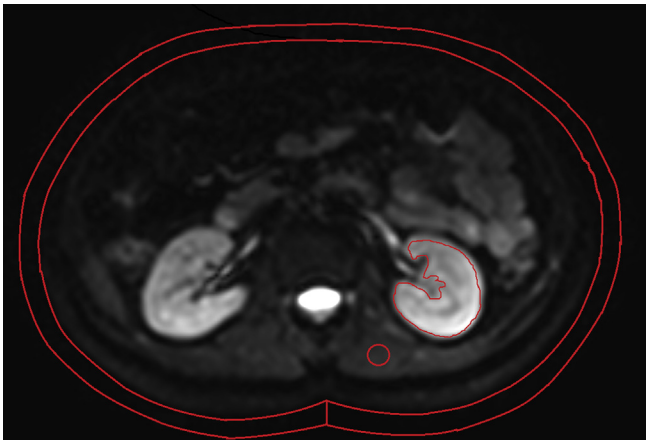

Figure 1 Demonstration of regions of interest (ROI)s in the renal parenchyma, background air, and muscle on b=0 images of iShim ss-EPI DWI. ROIs for the kidney were delineated carefully within the margin of renal parenchyma at the level of renal hilum and the ROIs for background noise and muscle were drawn within the same slice.

compare differences in image quality parameters between SMS and iShim sequences, the distribution of data was first evaluated with the Kolmogorov–Smirnov test, and then the paired *t*-test was used to compare normally distributed data otherwise the Wilcoxon signed-rank test was used. Inter-observer agreement for subjective and objective image quality assessments were analysed by using Cohen's kappa efficiency and intra-class correlation coefficient (ICC) respectively. ICC values were interpreted according to Kundel and Polansky[22]: 0.81–1.00, excellent; 0.61–0.80, good; 0.41–0.60, moderate; 0.21–0.40, fair; 0.00–0.20, poor. The distribution and concordance of ADCs between SMS and iShim sequences were shown in a Bland–Altman plot. The mean percentage difference and 95% limits of agreement between the two sequences were reported.

Results

Data were successfully acquired for all the 28 candidates and no data had to be excluded for analysis. Five axial b-value images acquired with SMS and prototypic ss-EPI sequence with an iShim sequence are shown in Fig 2. The scan time for SMS and iShim DWI was 1 minutes 38 seconds and 3 minutes 33 seconds, respectively. The scan time of SMS DWI was significantly reduced in comparison to iShim DWI by 53%. The mean ROI size for the kidney, psoas muscle, and background noise were 21.32±5.04, 1.01±0.28, and 40.01±6.32 cm^2 respectively. Table 2 shows the inter-observer agreement for each subjective and objective image quality parameter for SMS and iShim DWI. For subjective image quality assessment, most parameters were in good or excellent interobserver agreement for both sequences (kappa 0.624–0.873), but overall image quality and artefacts on b=0 images for both sequences, distortion on b=0, b=80 images for SMS, and b=400 images for iShim DWI showed moderate interobserver agreements (kappa 0.425–0.602). For objective image quality assessment, SNR and CNR of all b-value images were in good to excellent interobserver agreement (ICC: 0.736–0.996 for SMS, 0.758–0.992 for iShim). The mean ADC value of all the subjects was $(1.54\pm0.11)\times10^{-3}$ mm^2/s for SMS and $(1.52\pm0.16)\times10^{-3}$ mm^2/s for iShim sequences and there was no significant difference between them (p=0.343, Wilcoxon signed-rank test). The Bland–Altman plot shows that only one pair of samples lies beyond the 95% limits of agreement in ADC between iShim and SMS, and mean difference in percentage and limits of agreement in ADC between the two sequences is −1.3% (95% confidence interval [CI]: −15.8–13.1%; Pearson's correlation coefficient: 0.672, $p<0.0001$), indicating a high concordance between iShim and SMS (Fig 3). The ADC value between participants with normal eGFR (>90 ml/min/1.73m^2; n=10) and patients with decreased eGFR (<90 ml/min/1.73m^2; n=18) were analysed

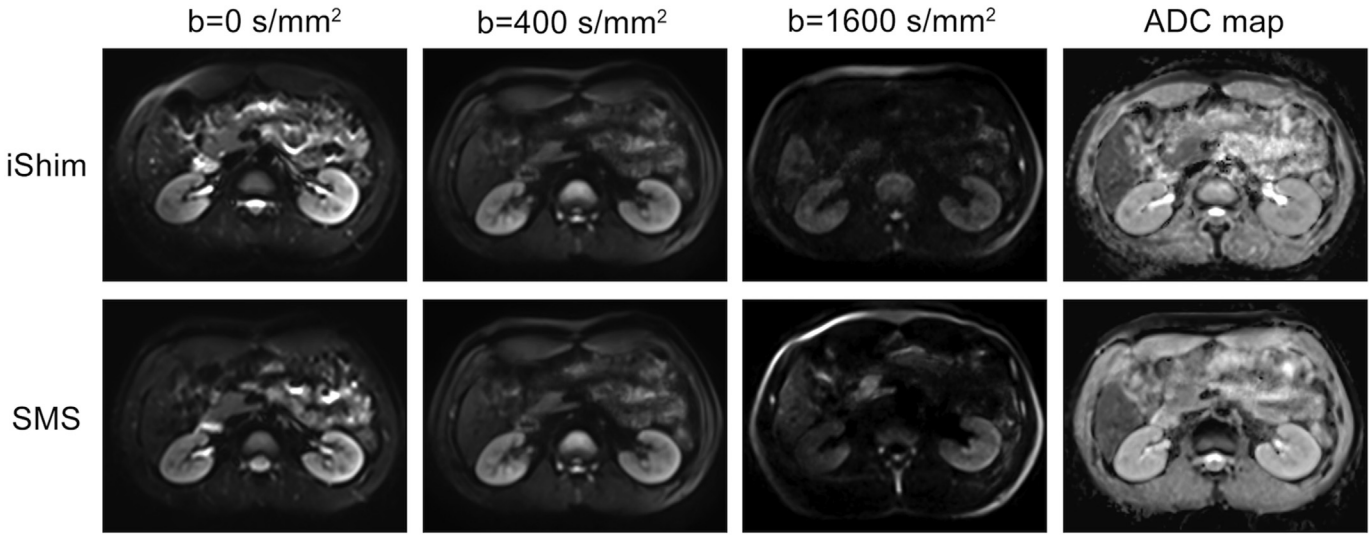

Figure 2 Comparison of SMS and iShim DW images. Axial DWI images of a healthy volunteer acquired with SMS (lower row) and prototypic ss-epi sequence with an iShim sequence (upper row).

Table 2
Interobserver agreement for each image quality parameter for each sequence.

b-Value (s/mm^2)	SMS					iShim				
	Overall IQ	Artefacts	Distortion	SNR[a]	CNR[a]	Overall IQ	Artefacts	Distortion	SNR[a]	CNR[a]
0	0.478	0.602	0.565	0.822	0.996	0.425	0.565	0.624	0.758	0.981
80	0.639	0.691	0.586	0.830	0.990	0.739	0.730	0.664	0.777	0.992
400	0.723	0.763	0.705	0.956	0.736	0.731	0.731	0.600	0.985	0.991
800	0.696	0.873	0.709	0.977	0.931	0.770	0.837	0.717	0.912	0.854
1,600	0.678	0.819	0.736	0.932	0.936	0.791	0.866	0.872	0.949	0.954

IQ, image quality; SNR, signal-to-noise ratio; CNR, contrast-to-noise ratio.
[a] Data are intraclass correlation coefficients and other data are kappa values.

further, and the results showed that the ADC value was significantly lower in patients with impaired renal function (SMS: $(1.51\pm0.18)\times10^{-3}$ versus $(1.64\pm0.15)\times10^{-3}$ mm^2/s, $p<0.001$, Wilcoxon signed-rank test; iShim: $(1.48\pm0.14)\times10^{-3}$ versus $(1.65\pm0.11)\times10^{-3}$ mm^2/s, $p<0.001$, Wilcoxon signed-rank test).

Subjective image quality assessment

Table 3 gives an overview of subjective image quality evaluation for the two sequences. For overall image quality evaluation, all the images of the SMS sequence and corresponding ADC map were rated >3, but some b=1,600 images of the iShim sequence were given a score of 2. Except on b=0 images where two sequences had similar score, SMS sequence had a significantly higher score of overall image quality on all the other b-value images and ADC map compared to the iShim sequences. Regarding artefacts, differences were noticed on b=80 and 800 images and ADC maps. Artefacts were more pronounced in iShim-DWI compared to SMS-DWI. There was similar presence of artefacts on b=0, 400, and 1,600 images between the two sequences. For image distortion, most images had no or mild distortion for both sequences and distortion was more obvious in the pole of the kidney. No significant differences were observed on all the b-value images between SMS and iShim sequences, but the ADC map of SMS showed less image distortion compared to the iShim sequence (SMS versus iShim: 4.52±0.54 versus 4.25±0.55, p=0.007, Wilcoxon signed-rank test).

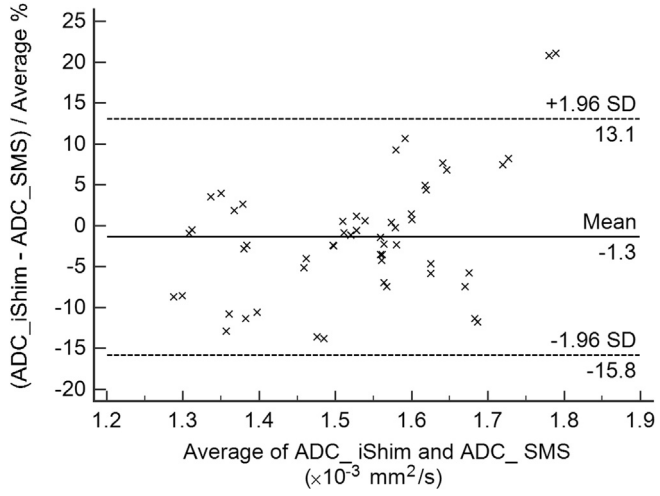

Figure 3 Bland–Altman plot for the ADCs between SMS and iShim sequences. There is only one pair of samples beyond the 95% limits of agreement in ADC between iShim and SMS, indicating the high accordance of ADCs between the two sequences.

Objective image quality assessment

Table 4 shows detailed results of the SNR and CNR on b-value images and ADC maps for both sequences. Except on b=0 images, the SNR was significantly higher on other b-value images and ADC map in SMS sequence. On b=0 images, no significant difference in SNR was noted between the two sequences, but CNR was significantly lower in SMS sequences. On the contrary, the CNR was significantly higher in SMS sequences on b=1,600 images. There were no significant differences in CNR on other b-value images and ADC map between SMS and iShim sequences.

Discussion

In the present study, a comparison between SMS and iShim DWI of the kidney with regard to image quality and scan time was performed. A substantial reduction in acquisition time to less than a half of the original scan time was achieved by SMS DWI. Generally, overall image quality was rated higher in SMS than in iShim DWI whereas subjective evaluation of presence of artefacts or distortions were comparable between SMS and iShim DWI. Although there was no significant difference in CNR in most b-value images and ADC map, SNR was superior in SMS than in iShim DWI. Therefore, the present study indicates that the SMS sequence enables a much faster acquisition of kidney DWI with slightly improved image quality in comparison to the iShim ss-EPI sequence.

Previous studies have reported that iShim can improve image quality of DWI in the imaging region that has strong susceptibility artefacts, and scan time could be moderately reduced compared to a standard shim mode.[19] According to the present results, in terms of the scan time, it was relatively longer, but still within an acceptable range (mean scan time for iShim, 3 minutes 33 seconds). On the other hand, as the iShim sequence was designed to

Table 3
Subjective image quality assessment of SMS and iShim DWI.

Parameter	Sequence	b=0	b=80	b=400	b=800	b=1,600	ADC map
Overall image quality	SMS	4.29±0.49	4.46±0.50	4.54±0.54	4.21±0.53	3.52±0.60	4.23±0.50
	iShim	4.27±0.49	3.71±0.85	3.70±0.81	3.21±0.71	2.98±0.59	3.27±0.65
	p-Value[a]	0.782	<0.001	<0.001	<0.001	<0.001	<0.001
Artefact	SMS	4.34±0.48	4.39±0.65	4.29±0.68	4.21±0.62	3.54±0.63	4.41±0.63
	iShim	4.43±0.50	4.12±0.81	4.16±0.78	3.91±0.79	3.57±0.60	3.77±0.76
	p-Value[a]	0.317	0.039	0.279	0.031	0.740	<0.001
Distortion	SMS	4.61±0.49	4.50±0.54	4.61±0.56	4.36±0.52	3.66±0.58	4.52±0.54
	iShim	4.59±0.50	4.52±0.69	4.48±0.69	4.57±0.57	3.46±0.63	4.25±0.55
	p-Value[a]	0.841	0.874	0.280	0.056	0.097	0.007

[a] Significant difference is demonstrated at the 0.05 level with Wilcoxon signed rank test.

Table 4
Objective image quality assessment of SMS and iShim DWI.

Parameter	Sequence	b=0	b=80	b=400	b=800	b=1,600	ADC map
SNR	SMS	164±0.66	347±760	127±55.7	75.0±37.4	33.8±21.4	211±750
	iShim	150±0.61	121±52.3	83.7±31.0	53.9±28.4	21.0±8.39	57.2±97.3
	p-Value	0.209	<0.001	<0.001[a]	<0.001	<0.001	0.014
CNR	SMS	0.87±0.06	0.89±0.04	0.87±0.06	0.81±0.08	0.73±0.11	0.41±0.21
	iShim	0.89±0.06	0.89±0.06	0.86±0.10	0.79±0.15	0.66±0.15	0.41±0.21
	p-Value	0.018	0.535	0.683	0.619	0.002	0.707

Significant difference is demonstrated at the 0.05 level with Wilcoxon signed rank test unless otherwise indicated.
[a] Significant difference is demonstrated with paired *t* test.

improve image quality in regions with strong susceptibility of artefacts, application of iShim in the kidneys may not fully demonstrate the advantages of iShim in improving image quality. SMS has been shown to dramatically reduce scan time without negative effects on image quality in prior studies.[23,24] The present finding showed that a reduction of 53% in scan time was achieved by SMS (1 minute 38 seconds) compared to iShim DWI, which is in accordance with previous studies that SMS DWI could save more than half the original scan time.[12,25] SMS could contribute to a more efficient clinical workflow and make DWI part of the routine kidney MRI protocol. Conversely, the time saved with SMS may also be used for higher spatial resolution, more slices or acquisition schemes with a long acquisition time, such as intra-voxel incoherent motion (IVIM).

Interestingly, in the qualitative image quality analysis, SMS was found to be superior to iShim DWI in overall image quality, but comparable regarding the presence of artefacts and distortions. Although both sequences were integrated with the same image filter, kidneys still seem to have smoother margins and there seems to be less image noise in SMS DWI, which may explain the higher overall image quality but similar artefacts or distortions of SMS compared to iShim DWI. Although the reviewers were blinded to the DWI sequence when evaluating the image quality, it was still possible that they might have realised which kind of sequence they were reviewing as their impression for the two sequences may be slightly different, which is hard to avoid. This may also explain the better overall image quality, but comparable artefacts or distortions observed in SMS DWI.

In the quantitative comparison, the SNR of SMS was higher than that of iShim DWI except for b=0 images, but no significant difference in CNR was observed on most b-value images between SMS and iShim DWI. The difference in SNR between SMS and iShim DWI may be related to different fat-suppression techniques used in these two sequences (SMS: SPAIR, iShim: water excitation). There are other differences between SMS and iShim besides fat suppression techniques, thus it is not appropriate to conclude that SPAIR is superior to water excitation resulting in higher SNR of SMS DWI. In the present study, image noise was measured by using the SD of signal in air, which is a common way to evaluate the SNR. It is difficult to select appropriate ROIs for background noise as noise is not distributed uniformly in the background. To counteract such non-uniformity, ROIs were placed over the whole background to measure the background noise. This approach is not a perfect SNR measurement as it could be affected by artefacts, which were present in this study; however, the discrepancy between the SNR of SMS and iShim DWI was still demonstrated. The higher SNR is also in accordance with higher overall image quality in SMS.

The mean ADC of renal parenchyma was not significantly different between SMS and iShim DWI. It indicates the stability of ADC quantification in SMS DWI. Compared to previous studies, Yalcin-Safak *et al.*[26] reported lower ADC values of the renal parenchyma (1.2 versus 1.5×10^{-3} mm^2/s), but Kline *et al.*[27] reported higher ADC values of the renal parenchyma (2.2 versus 1.5×10^{-3} mm^2/s). As many factors can influence ADC values, such as field strength, b-values, and acquisition schemes, it is possible that different studies have slightly different ADC values. The present results are

consistent with previous studies that patients with impaired renal function have decreased ADC values of renal parenchyma compared to people with normal renal function.

There are several limitations to the study. First, the study only compared the image quality of SMS and iShim ss-EPI DWI of the kidney, and no comparison to other acquisition schemes was undertaken (such as segmented EPI or read-out segmented EPI); therefore, it remains unknown whether the image quality of SMS DWI would also be better than other EPI sequences. A systemic comparison between SMS and available commonly used DWI sequences may help to obtain a comprehensive understanding of the value of SMS. Second, all the data were acquired using a 3 T MRI system so it is not known whether the study results would be the same using a 1.5 or 7 T MRI system. Third, although 22 of the 28 participants were patients with renal diseases, they did not have any focal renal lesions, but rather smaller kidneys or loss of corticomedullary differentiation (CMD), and as the study was focused on evaluating the image quality, assessment of focal lesion conspicuity was not performed in the study. Besides, the sample size was relatively small and did not allow for valid assessment of SMS DWI for diagnosing renal lesions. Further studies with larger sample sizes are needed to investigate the ability of SMS to evaluate different focal renal diseases. Fourth, 11 patients had CKD and it was difficult to clearly differentiate the cortex from the medulla using DWI, thus in order to keep consistency across all the candidates, the ROIs were placed over the renal parenchyma instead of in the cortex or medulla separately. As loss of CMD is relatively common in patients with impaired renal function, measuring the parenchyma would be more appropriate considering real clinical situations.

In conclusion, SMS outperforms iShim ss-EPI for DWI of the kidney for a substantial reduction in scan time with slightly better image quality. ADC values of renal parenchyma measured in SMS DWI were comparable to in iShim DWI. The high image quality obtained with a much shorter scan time indicates SMS DWI may contribute to a more efficient workflow in clinical practice and great potential for applications in other diffusion schemes with long acquisition time, such as IVIM. Further studies are encouraged to investigate the clinical diagnostic performance of SMS DWI for evaluating different renal diseases.

Conflict of interest

All authors declare they have no conflict of interest.

Acknowledgements

This work was supported by grants from the Fundamental Research Funds for the Central Universities (grant no.: 3332018022 to H.S.), the Education reform fund of Peking Union Medical College (grant no.:10023201700104 to H.S.) and the National Public Welfare Basic Scientific Research Project of China (grant no.: 2017PT32004 to Z.Y.J).

Two authors (T.Q. and J.A.) are employees of Siemens. All the other authors declare no relationships with any companies, whose products or services may be related to the subject matter of the article.

References

1. Woo KT, Choong HL, Wong KS, *et al*. The contribution of chronic kidney disease to the global burden of major noncommunicable diseases. *Kidney Int* 2012;**81**:1044–5.
2. Chow WH, Dong LM, Devesa SS. Epidemiology and risk factors for kidney cancer. *Nat Rev Urol* 2010;**7**:245–57.
3. Grenier N, Merville P, Combe C. Radiologic imaging of the renal parenchyma structure and function. *Nat Rev Nephrol* 2016;**12**:348–59.
4. Ramamurthy NK, Moosavi B, McInnes MD, *et al*. Multiparametric MRI of solid renal masses: pearls and pitfalls. *Clin Radiol* 2015;**70**:304–16.
5. Caroli A, Schneider M, Friedli I, *et al*. Diffusion-weighted magnetic resonance imaging to assess diffuse renal pathology: a systematic review and statement paper. *Nephrol Dial Transplant* 2018;**33**:ii29–40.
6. Ko SF, Yip HK, Zhen YY, *et al*. Severe bilateral ischemic-reperfusion renal injury: hyperacute and acute changes in apparent diffusion coefficient, T1, and T2 mapping with immunohistochemical correlations. *Sci Rep* 2017;**7**:1725.
7. Cakmak P, Yagci AB, Dursun B, *et al*. Renal diffusion-weighted imaging in diabetic nephropathy: correlation with clinical stages of disease. *Diagn Interv Radiol* 2014;**20**:374–8.
8. Friedli I, Crowe LA, de Perrot T, *et al*. Comparison of readout-segmented and conventional single-shot for echo-planar diffusion-weighted imaging in the assessment of kidney interstitial fibrosis. *J Magn Reson Imaging* 2017;**46**:1631–40.
9. Inoue T, Kozawa E, Okada H, *et al*. Noninvasive evaluation of kidney hypoxia and fibrosis using magnetic resonance imaging. *J Am Soc Nephrol* 2011;**22**:1429–34.
10. Mao W, Zhou J, Zeng M, *et al*. Intravoxel incoherent motion diffusion-weighted imaging for the assessment of renal fibrosis of chronic kidney disease: a preliminary study. *Magn Reson Imaging* 2017;**47**:118–24.
11. Cornelis F, Tricaud E, Lasserre AS, *et al*. Multiparametric magnetic resonance imaging for the differentiation of low and high grade clear cell renal carcinoma. *Eur Radiol* 2015;**25**:24–31.
12. Kenkel D, Barth BK, Piccirelli M, *et al*. Simultaneous multislice diffusion-weighted imaging of the kidney: a systematic analysis of image quality. *Invest Radiol* 2017;**52**:163–9.
13. Weiss J, Martirosian P, Taron J, *et al*. Feasibility of accelerated simultaneous multislice diffusion-weighted MRI of the prostate. *J Magn Reson Imaging* 2017;**46**:1507–15.
14. Taron J, Martirosian P, Erb M, *et al*. Simultaneous multislice diffusion-weighted MRI of the liver: analysis of different breathing schemes in comparison to standard sequences. *J Magn Reson Imaging* 2016;**44**:865–79.
15. Filli L, Ghafoor S, Kenkel D, *et al*. Simultaneous multi-slice readout-segmented echo planar imaging for accelerated diffusion-weighted imaging of the breast. *Eur J Radiol* 2016;**85**:274–8.
16. Boss A, Barth B, Filli L, *et al*. Simultaneous multi-slice echo planar diffusion weighted imaging of the liver and the pancreas: optimisation of signal-to-noise ratio and acquisition time and application to intravoxel incoherent motion analysis. *Eur J Radiol* 2016;**85**:1948–55.
17. Wu W, Miller KL. Image formation in diffusion MRI: a review of recent technical developments. *J Magn Reson Imaging* 2017;**46**:646–62.
18. Breuer FA, Blaimer M, Heidemann RM, *et al*. Controlled aliasing in parallel im- aging results in higher acceleration (CAIPIRINHA) for multislice imaging. *Magn Reson Med* 2005;**53**:684–91.
19. Zhang H, Xue H, Alto S, *et al*. Integrated shimming improves lesion detection in whole-body diffusion-weighted examinations of patients with plasma disorder at 3 T. *Invest Radiol* 2016;**51**:297–305.
20. Walter SS, Liu W, Stemmer A, *et al*. Combination of integrated dynamic shimming and readout-segmented echo planar imaging for diffusion weighted MRI of the head and neck region at 3 Tesla. *Magn Reson Imaging* 2017;**42**:32–6.

21. Schick F, Forster J, Machann J, *et al*. Highly selective water and fat imaging applying multislice sequences without sensitivity to B1 field inhomogeneities. *Magn Reson Med* 1997;**38**:269–74.
22. Kundel HL, Polansky M. Measurement of observer agreement. *Radiology* 2003;**228**:303–8.
23. Frost R, Jezzard P, Douaud G, *et al*. Scan time reduction for readout-segmented EPI using simultaneous multislice acceleration: diffusion-weighted imaging at 3 and 7 Tesla. *Magn Reson Med* 2015 Jul;**74**(1):136–49. https://doi.org/10.1002/mrm.25391.
24. Filli L, Piccirelli M, Kenkel D, *et al*. Simultaneous multislice echo planar imaging with blipped controlled aliasing in parallel imaging results in higher acceleration: a promising technique for accelerated diffusion tensor imaging of skeletal muscle. *Invest Radiol* 2015;**50**:456–63.
25. Taron J, Martirosian P, Schwenzer NF, *et al*. Scan time minimization in hepatic diffusion-weighted imaging: evaluation of the simultaneous multislice acceleration technique with different acceleration factors and gradient preparation schemes. *MAGMA* 2016;**29**:739–49.
26. Yalcin-Safak K, Ayyildiz M, Unel SY, *et al*. The relationship of ADC values of renal parenchyma with CKD stage and serum creatinine levels. *Eur J Radiol Open* 2016;**3**:8–11.
27. Kline TL, Edwards ME, Garg I, *et al*. Quantitative MRI of kidneys in renal disease. *Abdom Radiol (NY)* 2018;**43**:629–38.